EBSD characterization of deformed lath martensite in IF steel

Z Lv[1,2*], X Zhang[2], X Huang[2], N Hansen[2]

[1]Key Laboratory of Advanced Forging & Stamping Technology and Science (Ministry of Education of China), Yanshan University, Qinhuangdao 066004, China
[2]Section for Materials Science and Advanced Characterization, Department of Wind Energy, Technical University of Denmark, Risø Campus, DK-4000 Roskilde, Denmark

*E-mail: zqlv@ysu.edu.cn

Abstract. Rolling deformation results in the transformation of a lath martensite structure to a lamellar structure characteristic to that of IF steel cold-rolled to medium and high strains. The structural transition takes place from low to medium strain, and electron backscatter diffraction analysis shows that the frequency of medium angle boundaries with misorientation angles of 5-10º decreases with increasing strain, while the frequencies of boundaries with angles in the ranges of 1-5º and 10-25º increase, resulting in the evolution of a bimodal misorientation angle distribution. The microstructural evolution and the strength are characterized for lath martensite rolled to a thickness reduction of 30%, showing that large changes in the misorientation take place, while the strain hardening rate is low.

1. Introduction

Martensitic transformation (MT) is an efficient grain refinement process, which introduces high densities of high angle boundaries, low angle boundaries and dislocations. Ferrous martensite shows a variety of morphologies [1-3], namely lath, butterfly, lenticular and thin plate shapes. Among these, lath martensite (LM) has the most obviously industrial significance because it appears in quenched commercial steels, such as plain low-carbon steels, low-carbon and low-alloy steels, maraging steels, and interstitial free (IF) steels [3-5]. In low carbon (below 0.4 wt % C) steels, the martensitic structure is divided at decreasing scale into packets, blocks, sub-blocks and laths, as shown in figure 1. In the case of the K-S orientation relationship, there are 24 variants (from V1 to V24), with different direction and parallel plane relationships in the martensitic structure (see reference [2] for the definition of the 24 variants). A packet consists of parallel blocks [3], and the laths in the blocks of a given packet can have up to 6 variants (e.g. V1-V6), with different parallel direction relationships on the same conjugate parallel close packed plane [2, 3, 6]. Each block consists of laths of two specific K-S variant groups (sub-blocks), which are misoriented by small angles of about 10 degrees, such as V1 and V4, V2 and V5, and V3 and V6 [2, 3].

Plastic deformation (PD) is another efficient grain refinement process that can further improve the mechanical properties of metallic materials. A combination of MT and PD can further enhance the grain refinement, however, the hardening behavior of LM is different from that of the ferrite structure, especially at low strains [7]. Huang et al. found that the hardness of deformed LM increases by < 10% after cold rolling to 30%, whereas the hardness of deformed ferrite (with different original grain sizes)

increases by 60 ~ 80% after a similar deformation strain [7]. There is a transition range at low strains (< 30%) where the work hardening is limited. It is therefore important to analyze the structural evolution of martensite during the early stages of cold rolling.

The present study follows previous research [7], with an aim of characterizing the deformed LM martensite at low strains (up to 30% rolling reduction) using electron backscatter diffraction (EBSD). The structure evolution is analyzed based on the changes of misorientation angles, as obtained from the EBSD data, and the evolution of mechanical properties with deformation is discussed.

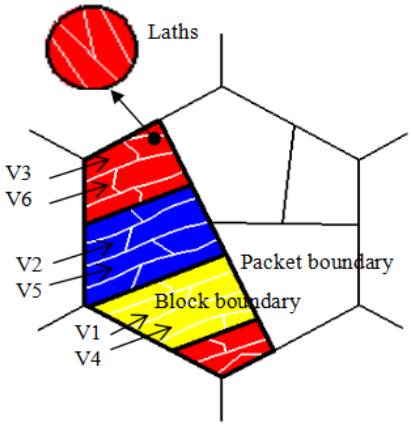

Figure 1. Schematic illustration showing a typical lath martensite structure in low carbon (0-0.4%) steels.

2. Material and experimental procedures

An IF steel (0.0026 C, 1.48Mn, 0.046Ti, 0.015Al, 0.0026 B, Fe balance, mass %) was used in this study. After austenitizing at 1473 K for 0.6 ks, specimens were quenched into iced brine to obtain a LM structure. The specimens with LM structure were cold rolled (CR) to 10% and 30% thickness reductions. Microstructures were characterized using a Zeiss Supra-35 scanning electron microscope (SEM) equipped with an Oxford Instruments EBSD detector. The SEM was operated at 20 kV. For the EBSD measurements, the samples were prepared by mechanical grinding and polishing with a final step using 1.0 μm diamond paste. The samples were then electrochemically polished at 30 kV for 20s in a methanol solution with 10 vol% perchloric acid. The EBSD maps were taken using a step size of 0.2 μm. Orientation data were collected using the Channel 5 acquisition software. Misorientation angles were calculated for statistical analysis where the misorientation angles of < 1º were excluded considering the angular resolution of the EBSD technique. To allow reliable statistics data for more than 1000 misorientation angles were collected in different areas of the EBSD maps for each sample.

3. Results and discussion

3.1 Un-deformed martensite

Here we use an inverse pole figure (IPF) coloring in the EBSD maps to show the microstructure of the initial sample without deformation, as shown in figure 2. The boundaries of the prior austenite grains (black lines), packets (blue lines) and blocks (red lines) can all be identified; an example is shown in figure 2b.

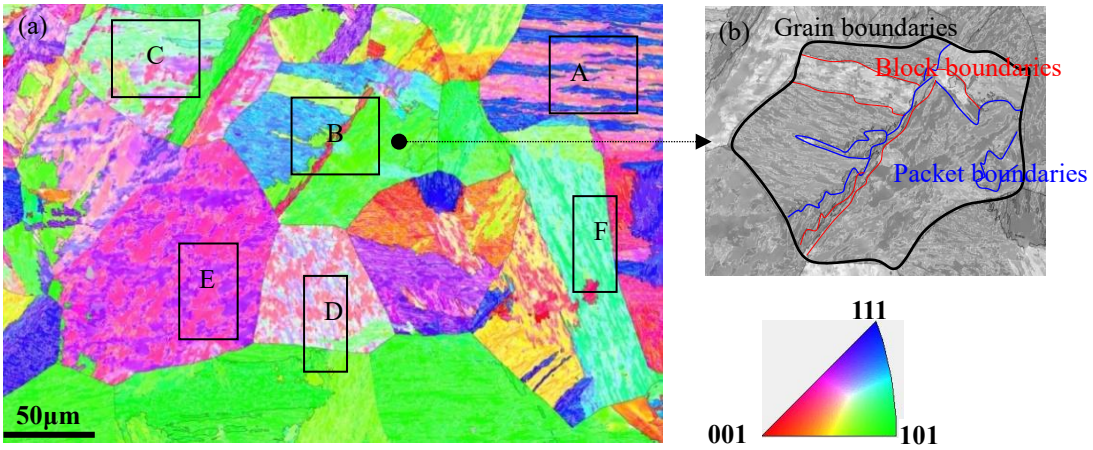

Figure 2. EBSD map of the un-deformed as-transformed martensite.

Figure 3a shows the distribution of misorientation angles between the 24 variants in the un-deformed LM. The misorientation angles between neighboring points were collected within individual prior austenite grains in the areas marked by A, B and C in figure 2a. Figure 3b lists the misorientation angles between V1 and other variants (V2-V24) forming the K-S orientation relationship [2]. If martensite variants are randomly distributed during the lath martensite formation process, boundaries with misorientation angles of > 15º should be much more frequent than boundaries with misorientation angles of <15º, as shown in figure 3b. However, the measured frequency of high angle boundaries is much smaller than the frequency of medium angle boundaries in the present case, as shown in figure 3a. The percentage of misorientations between 5-10º is about 24 %, which indicates the presence of a high number of sub-block boundaries (such as pairs with V1 and V4, V2 and V5, and V3and V6) in the LM, in agreement with previous observations [2,3,7].

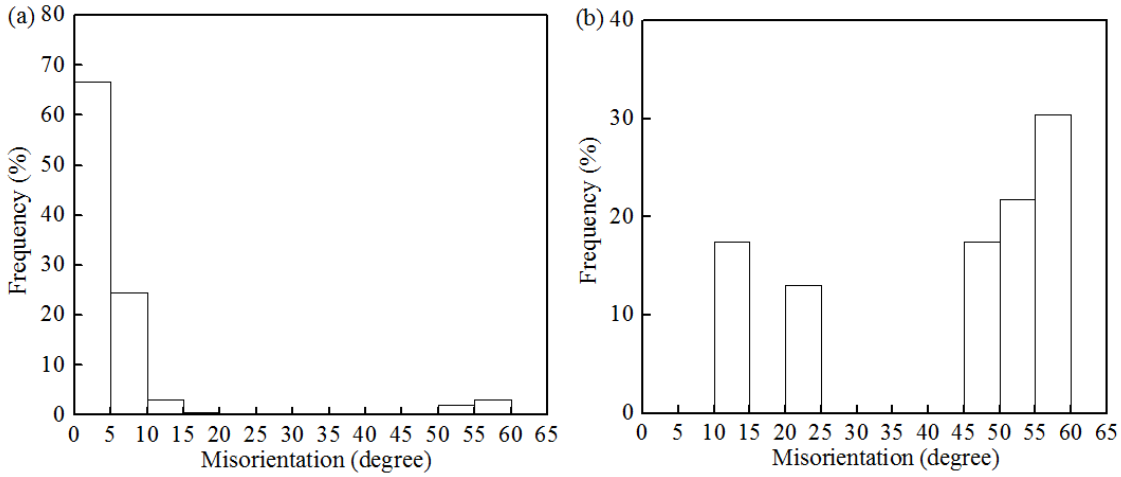

Figure 3. Misorientation angle distribution in un-deformed martensite: (a) from EBSD maps, excluding prior austenite grain boundaries; (b) between V1 and other variants (V2-V24) based on the K-S orientation relationship.

The misorientation angles between neighboring points were also measured in different blocks (such as areas D, E and F as marked in figure 2a). The resulting misorientation distribution based on all the measurements is shown in figure 4. The experimental results show the presence of sub-block boundaries

represented by a weak peak at 7º to 8º in the un-deformed LM, which agrees with previous findings [7]. The percentage of misorientations below 5º, related to the lath boundaries, is 70%, and that from 5º to 15º, related to sub-block boundaries, is 30%.

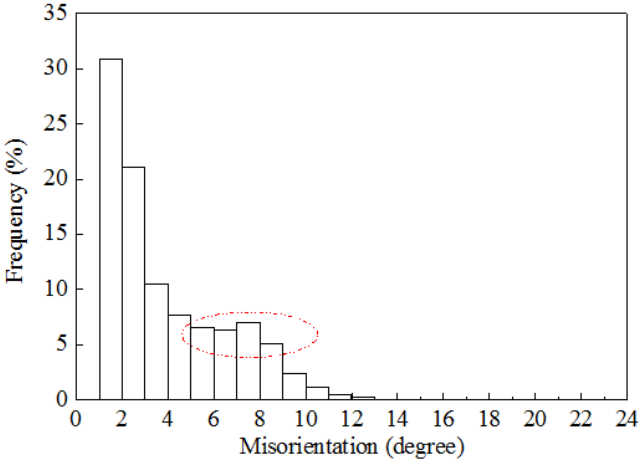

Figure 4. Misorientation distribution in blocks of un-deformed LM (excluding block boundaries).

3.2. Deformed microstructure

Figure 5 shows example EBSD maps of deformed martensite after 10% and 30% cold rolling. The rolling introduces some deformed structure, seen in area H of figure 5a and in area M of figure 5b, and is most pronounced in the 30% cold-rolled sample, where a certain structural alignment can be observed. The effect of cold rolling to low-strain on the shape of the prior austenite grains is observed to be small.

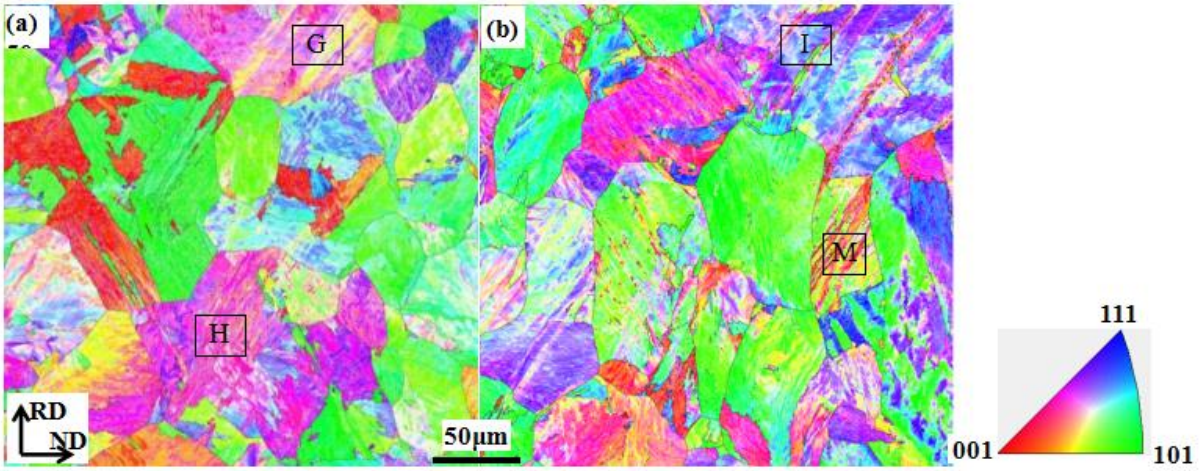

Figure 5. EBSD maps of cold rolled martensite: (a) 10% and (b) 30% thickness reduction.

Figure 6 shows the misorientation distribution from EBSD maps of the deformed LM after 10% and 30% cold rolling. The misorientation angles between neighboring points area again collected only from within the prior austenite grains.

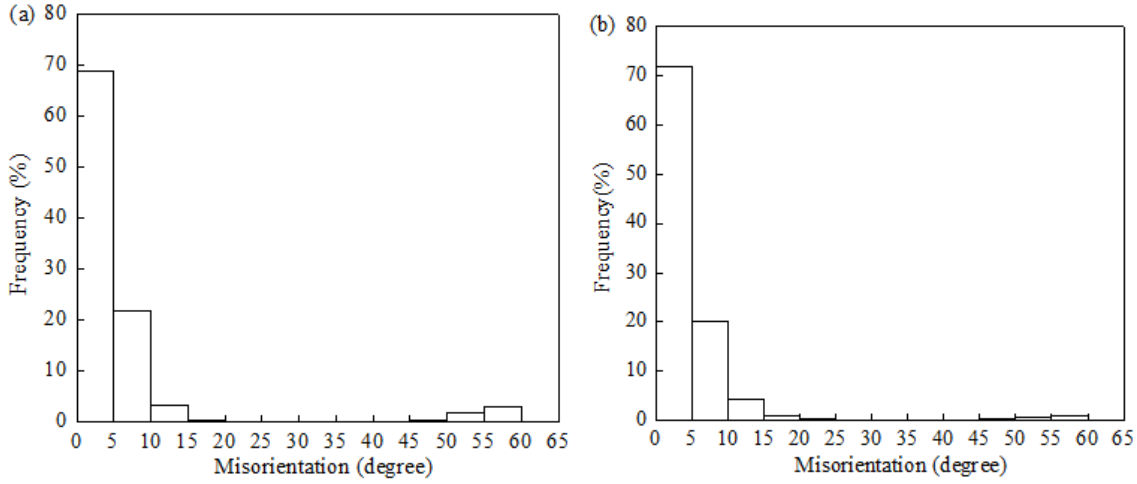

Figure 6. Misorientation distribution of deformed LM: (a) 10% CR. and (b) 30% CR.

The distributions of misorientation angles measured within different blocks at the two rolling reductions (such as areas G, H, I, and M in figure 5), considering all misorientations >1º, are illustrated in figure 7. The results show that high misorientation angles appear after 10% and 30% cold rolling. Misorientation angles up to 17º are observed in the 10% CR sample and to about 21º in the 30% CR sample. The percentage of misorientations below 5º is 68%, from 5º to 10º about 27%, and above 10º about 5% in the 10% cold-rolled sample. In the 30% CR sample, the percentage of misorientations below 5º is 74%, from 5º to 10º about 20%, and above 10º about 6%. The frequency of medium angles (5-10º) gradually decreases with increasing rolling reduction, and is accompanied by an increase in the frequency of lower (1-5º) and higher (> 10º) angles in the blocks.

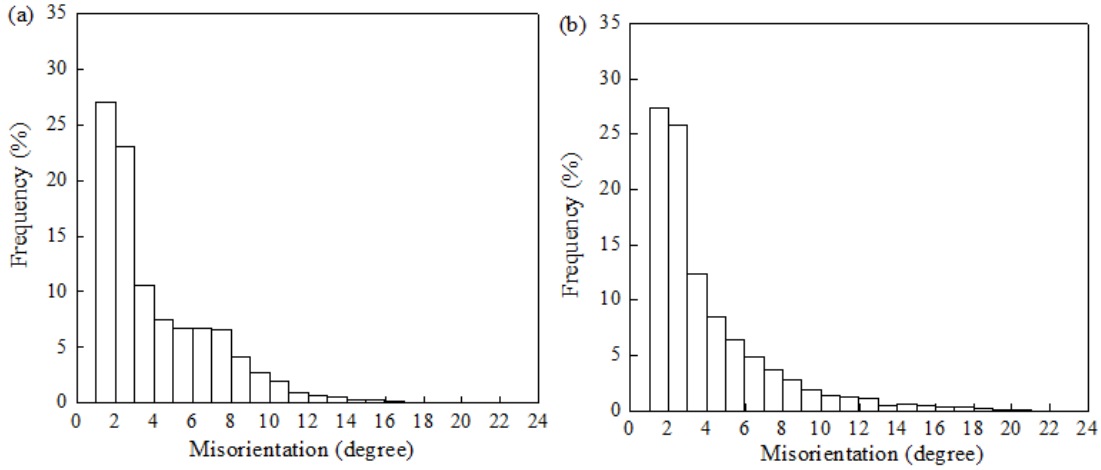

Figure 7. Misorientation distribution in blocks of deformed martensite (a) 10 % CR, (b) 30 % CR.

4. Discussion

The changes in structure and strength of lath martensite when cold rolled up to 80% ($\varepsilon_{vM} = 1.86$) have been analyzed in a recent paper [7]. It was found that the martensite structure broke down and transformed into a lamellar cell block structure characteristic of plastically deformed bcc and fcc metals [8-11]. It was also found that changes in strength are small for reductions up to 30%, followed by a stage

of almost constant hardening rate typically characteristic of stage IV hardening [12]. The previous structural analysis based on transmission electron microscopy (TEM) is in the present study replaced by the EBSD analysis, covering only the transition region up to a rolling strain of 30%. In parallel to the structural analysis, the changes in flow stress and hardness have been determined. The structural analysis shows significant changes in the distribution of misorientation angles across dislocation boundaries that subdivide the martensite structure, with the fraction of boundaries with misorientation angles 5-10º decreasing and the fractions of boundaries of smaller angle (1-5º) and larger angles (10-25 º) increasing with increasing cold-rolling reduction, as shown in table 1.

Table 1. Percentage of misorientation angles in different ranges in the LM samples

Sample	1-5° (%)	5-10° (%)	10-25° (%)	25-45° (%)	45-65° (%)
Ideal K-S OR	0	0	30.4	0	69.6
Un-deformed LM	66.7	24.5	3.5	0	5.3
10% CR	68.9	21.8	3.8	0.1	5.4
30% CR	71.8	20.1	5.8	0.1	2.2

The misorientation angle distribution thereby evolves towards a bimodal distribution characteristic of bcc and fcc metals rolled to medium and high strains [13]. The strength analysis (not shown here) shows a relative small increase in hardness and flow stress in the transition region (0-30% thickness reduction). The hardening rate is low and of the same order as observed previously in martensite and IF steel rolled to reductions in the same range [7]. It can be assumed that the strengthening mechanisms in rolled martensite primarily are dislocation strengthening and boundary strengthening. It should be noted, however, that the contribution of these mechanisms to the strength cannot be quantified exactly based only on EBSD data, as they exclude dislocation boundaries with an angle < 1°. Qualitatively, however, the changes in the misorientation angle distribution during rolling suggest that contributions from both hardening mechanisms may increase, but not to a large extent. The evolution of structure and strength of martensite when rolled up to 30% shows a near balance of hardening and softening mechanisms. The hardening mechanisms relate to an increase in the misorientation angle across dislocation boundaries and to a decrease in boundary spacing. This will lead to strengthening, which is counteracted by dislocation annihilation and boundary removal, e.g. by triple junction motion [14]. The result is a remarkable structural change with only a small effect on the strength and the strain hardening behavior. The contributions of hardening and softening mechanisms in the transition region are under investigation by EBSD and TEM, but a major challenge is the structural heterogeneity caused by the operation and interaction of dislocation glide processes, which affects the microstructural evolution, where an example is the formation of micro-shear bands observed as S-bands [12,13].

5. Conclusions

An IF steel with a lath martensite structure has been cold rolled 10% and 30% thickness reductions and the structural evolution has been followed by EBSD analysis. The following conclusions can be drawn.

(1) The frequency of medium angle boundaries (5-10º) in martensite blocks decreases with increasing strain, while the frequencies of boundaries of smaller angles (1-5º) and of larger angles (> 10º) increase. The overall result is the evolution towards a bimodal misorientation angle distribution, characteristic for IF steel rolled to medium and large strains.

(2) The structural morphology changes from a lath martensite structure to a lamellar cell block structure characteristic of cold rolled IF steel. The strain hardening rate is low and the experiment demonstrates that significant structural changes can take place with only a limited effect on the flow stress and hardness. This can be understood in terms of a balance between strain hardening and dynamic

softening by recovery.

Acknowledgements
The authors would like to thank D. Juul Jensen for many helpful discussions. This work was supported by the Natural Science Foundation of Hebei Province for Distinguished Young Scholar (E2017203036).

References

[1] Maki T 1990 *Mater. Sci. Forum* **56-58** 157
[2] Morito S, Tanaka H, Konishi R, Furuhara T and Maki T 2003 *Acta Mater.* **51** 1789-1799
[3] Morito S, Huang X, Furuhara T, Maki T and Hansen N 2006 *Acta Mater.* **54** 5323-5331
[4] Krauss G and Marder A R 1971 *Metall. Trans. A* **2** 2343-2347
[5] Maki T, Tsuzaki K and Tamura I 1980 *Trans. ISIJ* **20** 207-211
[6] Stormvinter A, Miyamoto G, Furuhara T, Hedstrom P and Borgenstam A *2012 Acta Mater.* **60** 7265-7274
[7] Huang X, Morito S, Hansen N and Maki T 2012 *Metall. Mater. Trans. A* **43** 3517-3531
[8] Hughes D A and Hansen N 2000 Acta Mater. **48** 2985-3004
[9] Li B L, Godfrey A, Meng Q C, Liu Q and Hansen N 2004 Acta Mater. **52** 1069
[10] Liu Q, Huang X, Lloyd DJ, Hansen N 2002 Acta Mater. **50** 3789
[11] Zhang X, Hansen N, Gao Y and Huang X 2012 *Acta Mater.* **60** 5933
[12] Hansen N 2001 *Metall. Mater. Trans. A* **32** 2917-2935
[13] Hughes D A and Hansen N 1997 *Acta Mater.* **45** 3871
[14] Yu T, Hansen N, Huang X and Godfrey A 2014 *Mater. Res. Lett.* **2** 160